

Demonstration of ultra-wideband (UWB) over fiber based on optical pulse-injected semiconductor laser

Yu-Shan Juan and Fan-Yi Lin*

*Institute of Photonics Technologies, Department of Electrical Engineering,
National Tsing Hua University, Hsinchu 300, Taiwan*

*fylin@ee.nthu.edu.tw

Abstract: We experimentally demonstrated the ultra-wideband (UWB) signal generation utilizing nonlinear dynamics of an optical pulse-injected semiconductor laser. The UWB signals generated are fully in compliant with the FCC mask for indoor radiation, while a large fractional bandwidth of 93% is achieved. To show the feasibility of UWB-over-fiber, transmission over a 2 km single-mode fiber and a wireless channel utilizing a pair of broadband antennas are examined. Moreover, proof of concept experiment on data encoding and decoding with 250 Mb/s in the optical pulse-injected laser is successfully demonstrated.

© 2010 Optical Society of America

OCIS codes: (140.5960) Semiconductor lasers; (190.3100) Instabilities and chaos; (060.5625) Radio frequency photonics; (140.3520) Injection-locked.

References and links

1. D. Porcine, P. Research, and W. Hirt, "Ultra-wideband radio technology: potential and challenges ahead," *IEEE Commun. Mag.* **41**, 66–74 (2003).
2. Federal Communications Commission, "Revision of part 15 of the commissions rules regarding ultra-wideband transmission systems," (2002)
3. Q. Wang, F. Zeng, S. Blais, and J. Yao, "Optical ultrawideband monocycle pulse generation based on cross-gain modulation in a semiconductor optical amplifier," *Opt. Lett.* **31**, 3083–3085 (2006).
4. J. Li, Y. Liang, and K. K. Y. Wong, "Millimeter-wave UWB signal generation via frequency up-conversion using fiber optical parametric amplifier," *IEEE Photon. Technol. Lett.* **21**, 1172–1174 (2009).
5. F. Zeng and J. P. Yao, "An approach to ultra-wideband pulse generation and distribution over optical fiber," *IEEE Photon. Technol. Lett.* **31**, 823–825 (2006).
6. Q. Wang and J. Yao, "UWB doublet generation using nonlinearly biased electro-optic intensity modulator," *Electron. Lett.* **42**, 1304–1305 (2006).
7. M. Bolea, J. Mora, B. Ortega, and J. Capmany, "Optical UWB pulse generator using an N tap microwave photonic filter and phase inversion adaptable to different pulse modulation formats," *Opt. Express* **17**, 5023–5032 (2009).
8. J. Wang, Q. Sun, J. Sun, and W. Zhang, "All-optical UWB pulse generation using sum-frequency generation in a PPLN waveguide," *Opt. Express* **17**, 3521–3530 (2009).
9. M. Abtahi, M. Mirshafiei, J. Magne, L. A. Rusch, and S. LaRochelle, "Ultra-wideband waveform generator based on optical pulse-shaping and FBG tuning," *J. Lightwave Technol.* **20**, 135–137 (2008).
10. X. Yu, T. B. Gibbon, M. Pawlik, S. Blaaberg, and I. T. Monroy, "A photonic ultra-wideband pulse generator based on relaxation oscillations of a semiconductor laser," *Opt. Express* **17**, 9680–9687 (2009).
11. Y. S. Juan and F. Y. Lin, "Ultra broadband microwave frequency combs generated by an optical pulse-injected semiconductor laser," *Opt. Express* **17**, 18596–18605 (2009).
12. Y. S. Juan and F. Y. Lin, "Microwave-frequency-comb generation utilizing a semiconductor laser subject to optical pulse injection from an optoelectronic feedback laser," *Opt. Lett.* **34**, 1636–1638 (2009).
13. F. Y. Lin, S. Y. Tu, C. C. Huang, and S. M. Chang, "Nonlinear dynamics of semiconductor lasers under repetitive optical pulse injection," *IEEE J. Sel. Top. Quantum Electron.* **15**, 604–611 (2009).

14. E. K. Lau, X. Zhao, H. K. Sung, D. Parekh, C. Chang-Hasnain, and M. C. Wu, "Strong optical injection-locked semiconductor lasers demonstrating > 100 -GHz resonance frequencies and 80-GHz intrinsic bandwidths," *Opt. Express* **16**, 6609–6618 (2008).
 15. J. B. Jensen, R. Rodes, A. Caballero, X. Yu, T. B. Gibbon, and I. T. Monroy, "4 Gbps impulse radio (IR) ultra-wideband (UWB) transmission over 100 meters multi mode fiber with 4 meters wireless transmission," *Opt. Express* **17**, 16898–16903 (2009).
-

1. Introduction

Ultra-wideband (UWB) technology has attracted great interest recently for its advantages of high data rate, low power consumption, and immunity to multipath fading in short-range wireless communications [1]. Limited by the low emission power specified by the Federal Communications Commission (FCC) (a power density lower than -41.3 dBm/MHz) [2], the UWB signal can only transmit up to tens of meters in an indoor environment in a stand-alone mode. To extend the transmission distance, UWB-over-fiber topology adapting from the well-known radio-over-fiber systems may offer a feasible solution, which can also be integrated with the existing fixed wired networks and the wireless wide-area infrastructures. Therefore, to fully take the advantages of those cost-efficient photonic components commonly available in the optical fiber communications and to eliminate the need for extra electrical-to-optical conversion, generating the UWB signals directly in the optical domain is highly desirable.

Several optical approaches of UWB signal generation have been reported in the past few years. UWB pulse generations based on cross-gain modulation in semiconductor optical amplifier [3] and fiber optical parametric amplifier [4] have been demonstrated, where monocycle and doublet pulses with broad bandwidths have been generated. Generation of UWB pulse using electro-optic intensity modulator [5] and phase modulator [6] have also been shown. By utilizing phase inversion in a Mach-Zehnder modulator, optical UWB pulses have been generated with an N tap reconfigurable microwave photonic filter fed by a laser array [7]. An approach exploiting the parametric attenuation effect of sum-frequency generation for UWB pulse generation in a periodically poled lithium niobate waveguide has been investigated [8]. Other techniques based on optical pulse-shaping [9] and direct modulation and external injection in a semiconductor laser [10] have also been reported.

In this paper, we demonstrate the UWB signal generation and propose a UWB-over-fiber system based on an optical pulse-injected semiconductor laser. Without the need of expensive electro-optic modulator [5,6], pulse shaper [9], or laser array [7], UWB signals fully comply to the FCC mask with large fractional bandwidths can be generated utilizing the nonlinear dynamics of the laser. To show the feasibility of the UWB-over-fiber with the proposed scheme, the UWB signals transmitted through a 2 km single-mode fiber and a pair of broadband horn antenna are examined. Moreover, the proof of concept experiment of data encoding and decoding with the optical pulse-injected laser is also carried out.

2. Experimental Setup

Figure 1 shows the experimental setup of the proposed UWB-over-fiber system. The master laser (ML) and the slave laser (SL) are commercial single-mode distributed feedback semiconductor lasers with wavelengths of $1.3\ \mu\text{m}$ and relaxation frequencies of 7 GHz. The ML and SL lasers are biased at 30.7 mA and 24.0 mA and have optical power of about 8.5 mW and 7.3 mW, respectively. Optoelectronic feedback is utilized to generate the repetitive optical pulses in the ML [11, 12]. A 10 GHz photodetector (Albis PDCS65T) and a 3 GHz electric amplifier (JCA JCA003-201) are used in the feedback loop. By adjusting the length of the delay loop with the movable mirror and the feedback strength with the variable attenuator, pulses with different repetition frequencies f_{rep} can be obtained [11]. The UWB signals are generated by injecting

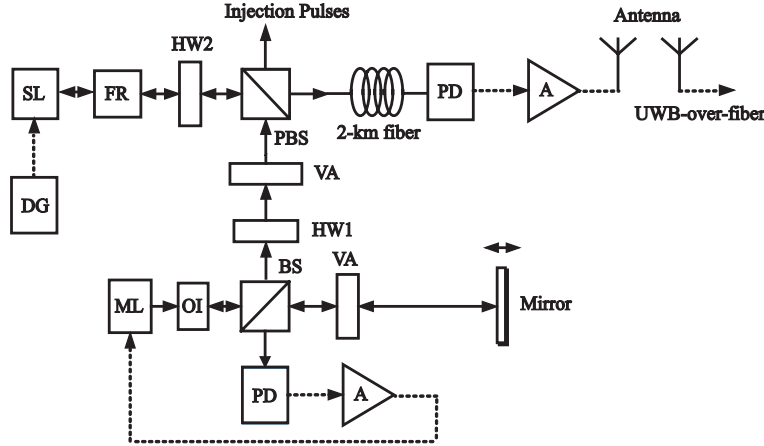


Fig. 1. Schematic setup of the UWB-over-fiber system. Optical pulses are generated by the master laser (ML) through optoelectronic feedback. The pulses are injected into the slave laser (SL) optically to generate the UWB signals. DG: data generator, PD: photodetector, OI: optical isolator, BS: beamsplitter, PBS: polarizing beamsplitter, HW: half-wave plate, VA: variable attenuator, FR: Faraday rotator, and A: amplifier. Solid and dashed lines indicate optical and electrical paths, respectively.

the optical pulses to the SL through a free space circulator formed by the half-wave plates, the polarizing beam splitter, and the Faraday rotator. UWB signals with large fractional bandwidths are obtained by tuning the operational parameters, which are the normalized injection strength ξ_i (the ratio of the output fields of the SL to the ML) and the detuning frequency Ω (the difference in optical frequencies between the ML and the SL). A 2 km single-mode fiber and a pair of broadband horn antenna (A-INFO JTXLB-10180) with bandwidths range from 1.0 to 18.0 GHz are used to demonstrate the UWB-over-fiber scheme. The output signals of the ML (injection pulses) and the SL (UWB signals) are detected by photodetectors (Discovery Semiconductors DSC30S) with amplifiers (MITEQ AFS6-00102000-30-10P-6) of 20 GHz bandwidths and recorded by a 26.5 GHz power spectrum analyzer (Agilent E4407B) and a 13 GHz real-time oscilloscope (LeCroy SDA13000). To encode the message, a data generator (Tektronix DG2030) is used to current modulate the SL.

3. Results and Discussions

Figures 2(a) and 2(b) show the power spectrum and the corresponding time series of the optical pulses generated from the ML subjected to the optoelectronic feedback. As can be seen, repetitive pulses with $f_{rep} = 0.9$ GHz and pulsewidths of 425 ps are generated. By adjusting the controllable parameters in the optoelectronic feedback loop, the repetition frequency can easily be tuned in a range of few GHz [11]. To generate the UWB signals, the optical pulses from the ML are injected into the SL. With the harmonic frequency components seen in Fig. 2(a) being the seeds, the UWB signals can be generated through redistributing the energies in each components by nonlinear frequency mixing [11]. Moreover, with the advantages of bandwidth enhancement through optical injection [14], UWB signals with large fractional bandwidths can be obtained.

Figures 3(a) and 3(b) show the power spectrum and the corresponding time series of the UWB signal generated in the SL by optical pulse injection with a line spacing of 0.9 GHz under $\xi_i = 0.23$ and $\Omega = 14.6$ GHz. Clearly, the generated UWB signal is in compliant with

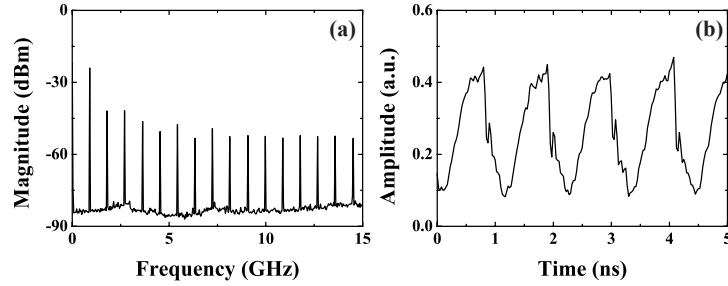


Fig. 2. (a) Power spectrum and (b) time series of the injection pulses from the ML with $f_{rep} = 0.9$ GHz.

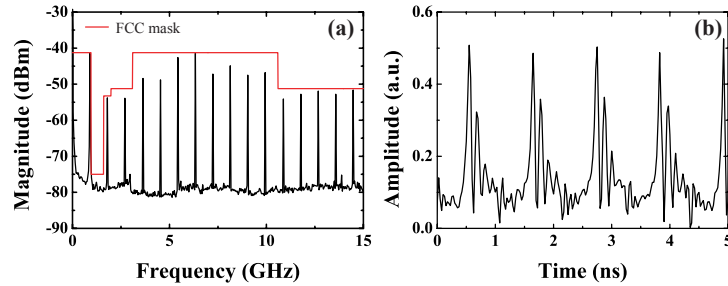


Fig. 3. (a) Power spectrum and (b) time series of the UWB signal generated by the SL through optical pulse injection with $f_{rep} = 0.9$ GHz, $\xi_i = 0.23$, and $\Omega = 14.6$ GHz.

the FCC mask for indoor radiation as shown in Fig. 3(a). The spectral envelope has a 10 dB bandwidth (within which the magnitudes of the frequency components differ by less than 10 dB to assure the continuity of the spectrum) of 6.3 GHz ranged from 3.6 to 9.9 GHz. As the result, a fractional bandwidth (the ratio between the 10-dB bandwidth to the center frequency) of 93%, well above the minimum requirement of 20% from the FCC, is successfully achieved. Compared with the benchmarks set by the direct modulation, external injection, and arbitrary waveform modulation schemes that have respective fractional bandwidths of 78%, 61%, and about 70% [10, 15], the UWB signal demonstrated clearly shows a significant improvement in the fractional bandwidth with the spectral envelope closely matches with the FCC mask. Moreover, utilizing optical pulse injection, the bandwidths of the UWB signals generated are not limited by the electronic bandwidth of the electrical components. Note that, fine tuning in the injection parameters is required for the phases of the frequency harmonic components to be stably locked and therefore produce UWB signals with lower noise floor and smaller amplitude fluctuation.

To examine the feasibility of UWB-over-fiber, a 2 km single-mode fiber and a pair of broadband horn antennas are used as the optical and wireless channels. Figures 4(a) and 4(d) show the respective power spectrum and the corresponding time series of the UWB signal transmitted over the 2 km fiber. Due to the loss and dispersion from the fiber, the magnitude of the spectral envelope becomes lower and the pulsewidths of the UWB pulses are broadened from 50 ps to about 100 ps, respectively. The power spectrum (calibrated to the antenna response) and the time series of the UWB signal transmitted through the antennas (back-to-back) are shown in Figs. 4(b) and 4(e), respectively. With the large dispersion in the antennas, the pulsewidths are greatly broadened to 950 ps. By considering both the fiber and the antennas, the power spectrum and the time series of the transmitted signal in the UWB-over-fiber configuration as shown

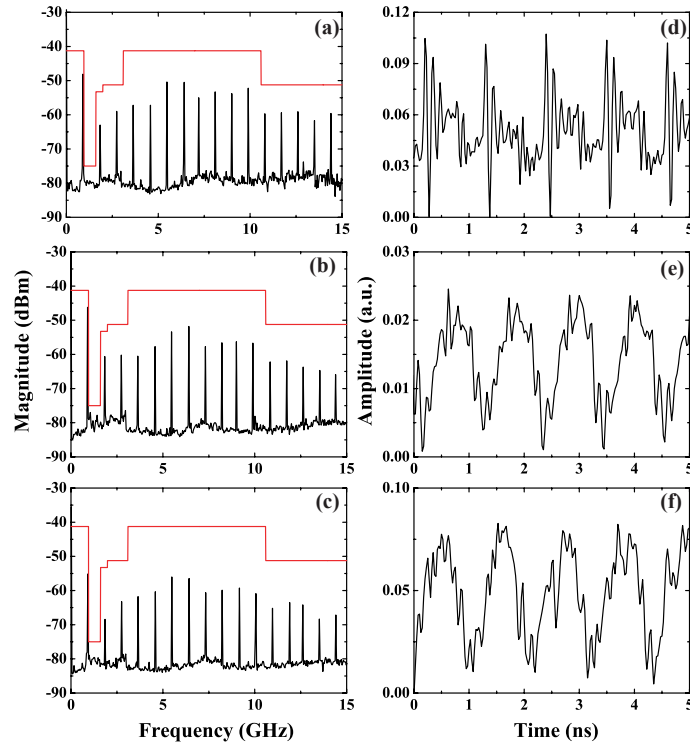


Fig. 4. (a-c) Power spectra and (d-f) time series of the UWB signal transmitted through a 2 km fiber, a pair of antenna (back-to-back), and both the fiber and the antennas, respectively.

in Fig. 1 are examined and shown in Figs. 4(c) and 4(f), respectively. While the power spectral densities at some frequencies are lower due to the excess loss after transmitting through both the optical and wireless channels, the spectral distribution is still in compliant with the FCC mask and the fractional bandwidth is successfully maintained at 93%.

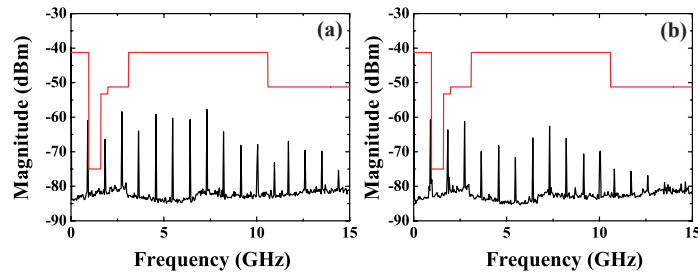


Fig. 5. Power spectra of the UWB-over-fiber transmission over a 2 km fiber and wireless channels of (a) 25 cm and (b) 75 cm, respectively.

By further increasing the distance between the antennas, Figs. 5(a) and 5(b) show the power spectra of the transmitted UWB signals over a 2 km fiber followed by a 25 cm and a 75 cm wireless transmission channels, respectively. As can be seen, as the distance between the antennas increases, the magnitude of the spectrum decreases due to the excess scattering and radiation loss. Nonetheless, the fractional bandwidths of the received UWB signals maintain at 93%.

Amplification may be needed at the receiver antenna to further extend the transmission range.

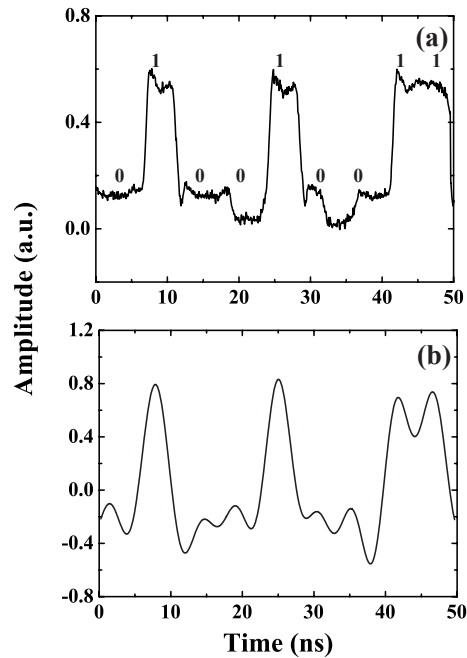


Fig. 6. (a) Encoded data and (b) Decoded data after low-pass filtering.

To demonstrate the capability of encoding and decoding in the optical pulse-injected laser, data sequence of “010010011” with a bit-rate of 225 Mb/s is applied at the SL through direct current modulation. By modulating the bias level, the dynamical states of the SL changes accordingly and are switched between the pulsing and non-pulsing states. Figure 6(a) shows the encoded data measured directly from the data generator, where a non-return-to-zero (NRZ) format is adopted. Figure 6(b) shows the decoded (received) data from the SL after low pass filtering. As can be seen, the exact data sequence is successfully recovered. Note that, limited by the data generator used, a bit-rate of 225 Mb/s is shown in this paper. The ultimate limitation in the bit-rate is limited by the repetition frequency of the injected pulses, which can be tuned in a range of few GHz by adjusting the delay time and the feedback strength in the optoelectronic feedback loop.

4. Conclusions

In conclusion, we have demonstrated and characterized the generation of UWB signals with an optical pulse-injected semiconductor laser. The UWB signals generated are fully in compliant with the FCC mask for indoor radiation. The fractional bandwidths as large as 93% are achieved, which are far beyond the minimum requirement of 20% defined by the FCC. Transmission of the UWB signal over a 2 km single-mode fiber and wireless channel utilizing a pair of antennas is realized. Moreover, the proof of concept experiment on data encoding and decoding with 250 Mb/s in the optical pulse-injected semiconductor laser is successfully demonstrated.

Acknowledgments

This work is supported by the National Science Council of Taiwan under contract NSC-97-2112-M-007-017-MY3.